COMPUTATIONAL AND EXPERIMENTAL STUDY OF OIL-WATER EMULSION FLOW AND STABILITY IN A STIRRED TANK

Amit V. PATIL[1*] and Stein T. JOHANSEN[1]

[1] SINTEF Material and Chemistry, S.P. Anderssen vei 15b, 7031, NORWAY
*Corresponding author, E-mail address: amit.patil@sintef.no

ABSTRACT

Oil-water emulsion flow behaviour was characterized with respect to surface chemistry. A state of the art stirred tank experimental set up was constructed that measured dynamic droplet size evolution with varying impeller speed. This technique was demonstrated with model Nexbase oil (with and without SPAN 80 surfactants) and water emulsions. Further, a CFD model for droplet size prediction was proposed. This model was tested for correct implementation and provides a tool for accommodating surface chemistry.

NOMENCLATURE

d droplet diameter
F phase interaction force
g gravity
t time
p pressure
$\mathbf{u}$ velocity
α phase fraction
μ dynamic viscosity
ρ density
τ tensor and time constant

Subscripts
d *dispersed phase*
c *continuous phase*
t *turbulent*

INTRODUCTION

The transport of crude oil and water emulsions is a key element in the flow assurance sector of the upstream oil and gas industries. The cost of crude oil production is strongly related to pressure drop produced in transport pipes. Further the pressure drop is dependent on stability characteristics of emulsions like interfacial tension and surface chemistry. Emulsions consist of dispersed droplets which either coalesce or break up depending on these characteristics. The prediction of the droplet size distribution is essential to determine flow behaviour and rheology of crude oil-water multi-phase flow.

It is well known that droplet size distribution under turbulent regime flows is governed by the Kolmogorov scale. The largest droplet size depends on interfacial stresses that are controlled by either the inertial or viscous stresses present as turbulent flow regimes (Kolmogorov 1949). The characterization of equilibrium droplet sizes with respect to interfacial stress regimes for varying oils and water was done extensively by previous researchers using stirred tank systems (Boxall et. al. 2012).

The droplet size in-situ measurements are done with techniques like particle video microscope (PVM) probe and Focussed beam reflectance measurement (FBRM) (Abdin 2013). However FBRM measures the cord lengths of droplets at its focus and hence require a re-calibration with PVM. Many works on calibration of FBRM has been done in the past so that online measurements can be made which is a unique feature of FBRM (Wynn 2003, Boxall et. al. 2010).

With recent advances in image processing techniques accurate measurement of dispersed shapes can be made using microscopy (Kempkes et. al. 2008). These processing methods could be implemented for measuring droplet size distribution from images captured by PVM. In this work we have developed such a measuring method that could be used for accurate droplet size evolution measurements with varying stirring speed of the impeller.

Knowing the set impeller speeds, interfacial tension and viscosity of continuous phase, the maximum droplet size stability can be obtained (Boxall et. al. 2012). However in oil-water emulsion studies where shear stress plays a major role it is important to measure the torque on the impeller. The measurement of droplet size alongside torque provides the exact influence of surface chemistry. We look to measure these influences and implement them as closures in Euler-Euler based models where droplet size is treated as a scalar quantity of the dispersed phase. This modelling method proposed here is motivated from previous work by Laux and Johansen (1999).

Modelling of emulsion turbulent flow in a stirred tank is well known and was done extensively by previous researchers (Ciofalo et. al. 1996), (Gohel et. al. 2012), (Murthy et. al. 2007). Most works in CFD have been about comparing advanced turbulence models (Murthy and Joshi 2008). But a CFD implementation that accounts for droplet stability and surface chemistry has not been attempted previously. This model was implemented in Fluent 15.0 where the geometry and its mesh were generated. Here we have used k-ε model for turbulence flow. In this model sliding mesh was used with cut impeller immersed boundary. This developed mesh was initially tested in a single phase flow. Next, it was extended with the multiphase model and tested.

EXPERIMENTAL METHOD

The jacketed tank has an internal diameter of 95mm and a height of 148mm. The capacity of the tank is 1265 mL. The input and output of the jacket is connected to an automatic temperature controller. The tank has two lateral entrances where the upper one is used for the PVM probe. The cross sectional view of this tank is shown in Fig. 1.

Baffles are placed inside the tank to avoid formation of vortices and increase shear in the system. The impeller used to do the experiments is a four flat blade impeller. Its diameter is 48 mm and the width is 10 mm. It is located at approximately 30 mm from the bottom of the tank. This design was chosen following the standard design of an agitated vessel (McCabe et. al. 2002).

The bottom of the tank was made slightly conical in shape tapering to the centre so that drainage and cleaning is easy. Baffles are part of a plate assembly attached to the lid. Both the lid and baffles are made of stainless steel so that they can withstand corrosion from oil and salt. The glass vessel is placed on a supported steel flange. The lid assembly covering the tank is clamped along with this steel flange. Rubber gasket was used between the rim opening of the glass tank and steel lid so that the glass is protected and there is no leakage. The assembled set up is shown in Fig. 2.
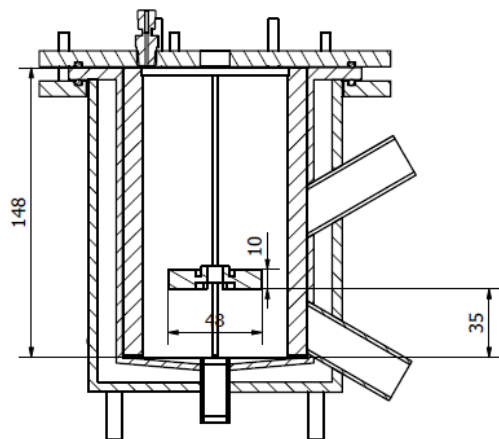
Figure 1: Schematic cross sectional view of jacketed stirred tank fitted with 4 baffles, openings for PVM probe, inlet and exits. It consists of a flat blade impeller with 4 blades. The diagram also provides dimensions of some essential parts in mm.

The stirred tank is mounted with Silverson L5M-A mixer that has a manual control of the impeller rotational speed. The shaft of the mixer connecting to the impeller is fitted with HBM 20WN torque sensor that accurately measures torque in the range of 0 to 5Nm. The sensor is aligned and connected with the shaft using a bellow coupling. This torque sensor is connected via an amplifier to computer recording system. The instantaneous measured torque during experimental runs is logged into the computer.

Alongside a PVM probe inserted into the tank captures high resolution images (1075μm x 825μm) of emulsion in the stirred tank. The PVM probe used was manufactured by Mettler Toledo Inc. These images are also logged with respect to time in the same computer system. These images are 1360pixel x 1024pixel in size which on calibration

was obtained to be 0.798 μm/pixel. The images are post-processed in MATLAB image processing tool box to obtain sizes of droplets. The images are initially smoothened using filters so that detection of rings becomes easy. The image processing software uses Otsu thresholding method to detect the edges (Otsu 1979). Further rings are detected using the Hough transform algorithm (Yuen et. al. 1990). Details of the processing are provided further in the results section. The frequency of image capture was set at 1/6 that is one image every 6 s.
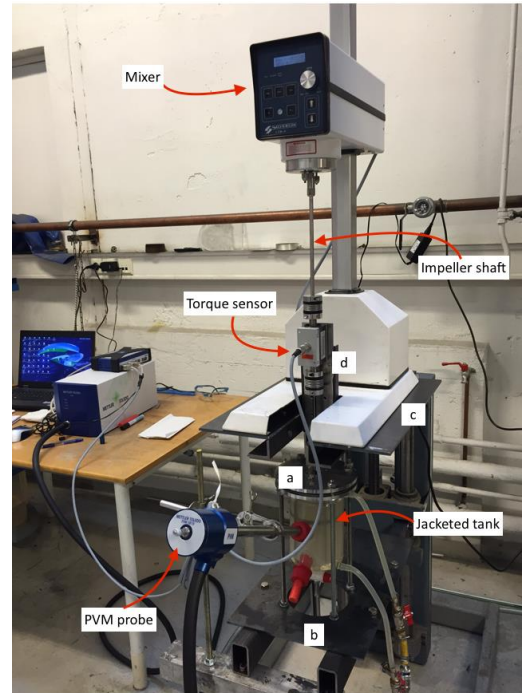
Figure 2: Image of stirred tank set up with all accessories. Other parts include (a): Sealing lid cover with temperature sensor. (b): Bottom plate support with level adjustment. (c): Mixer support. (d): Bellow coupling for impeller shaft with torque sensor.

The probe was inserted at about 4cm inside from the upper probe socket shown in Fig 1. The position of the probe was thus close to the middle about 4-5 cm away from the impeller. It is not known how the location of the impeller effects the droplet size distribution. It is anticipated that close to the impeller where the shear is high will show smaller droplet size compared to away from the impeller. This will be part of a future study. Here in these experiments only a base case for newly developed measuring technique is presented.

In these set of experiments model oil was chosen alongside tap water for the emulsion formation. The model oil phase was a mixture of NEXBASE®3080 oil (85% by wt) (a colourless, high purity isoparaffinic synthetic fluid comprising of hydrogenated C10 oligomers) which is a base oil provided by Neste Oil and toluene (15% by wt). Nexbase3080 was chosen simply because it is a clear transparent oil and provides clear interfaces with water. The water phase was prepared by mixing tap water with 3.5% NaCl salt making brine. The salt has a destabilization effect on the emulsions promoting improved oil-water separation. The fluid properties are summarized in Table 1.

Fluid	Density	Dynamic viscosity
	(g/ml)	(mPa.s)
Tap water (3.5% NaCl)	1.018	1.027
Nexbase 3080	0.798	5 at 40^{0}C
Toluene	0.87	1.25 at 20^{0}C
Nexbase 3080 (85%) + Toluene (15%)	0.842	-

Table 1: Fluid properties.

Two sets of experiments are reported here to show the effect of emulsion stability. In the first experiment 85% oil phase was emulsified with 15% water phase. Initially the rotation speed was kept high at 3500RPM for 120 s to cause break up and create small droplets. The rotation speed was relaxed instantly to 2000 RPM causing coalescence to reach a new equilibrium. This rotation speed is maintained for 240 s and then reduced further to 1000 RPM for 300 s. The rotation speed is again increased to 3500 RPM for 120 s before reducing it back to 1000 RPM.

Steps time (s)	Run 1 (without surfactants) (RPM)	Run 2 (with surfactants) (RPM)
120	3500	2500
240	2000	1500
300	1000	500
120	3500	2500
240	1000	500

Table 2: Impeller rotation speed sequences in experimental runs.

In the second experiment the oil phase is added with SPAN 80 surfactant (making 10ppm surfactant oil phase). The rotation speed variation pattern is the same but with different levels of rotation speeds (2500, 1500 and 500 RPM). These have been summarized in table 2. The droplet size distribution behaviour with time for both these experimental runs will be discussed in detail later in results section. Now we move to description of the computational model that was developed for prediction of droplet size evolution.

MODEL DESCRIPTION

Continuous phase

The oil water mixing creating a continuous and dispersed droplet phase undergo a turbulent flow behaviour in the given impeller speed ranges. The turbulence is modelled using Favre's averaging method. The continuity and momentum equations for the continuous phase are given by;

$$\frac{\partial \overline{\rho}_c}{\partial t} + \nabla \cdot \left(\overline{\rho}_c \tilde{\mathbf{u}}_c \right) = 0 \qquad (1)$$

$$\frac{\partial \overline{\rho}_c \tilde{\mathbf{u}}_c}{\partial t} + \nabla \cdot \left\{ \left(\overline{\rho}_c \tilde{\mathbf{u}}_c \tilde{\mathbf{u}}_c \right) + \left(\overline{\rho_c \mathbf{u}''_c \mathbf{u}''_c} \right) - \tau_c \right\} = -\alpha_c \nabla p + \overline{\rho}_c g - F_d \qquad (2)$$

Where,

$$\overline{\rho}_c = \alpha_c \rho_c$$

Dispersed phase

The dispersed phase is also modelled with continuity and momentum equations are given by;

$$\frac{\partial \overline{\rho}_d}{\partial t} + \nabla \cdot \left(\overline{\rho}_d \tilde{\mathbf{u}}_d \right) = 0 \qquad (3)$$

$$\frac{\partial \overline{\rho}_d \tilde{\mathbf{u}}_d}{\partial t} + \nabla \cdot \left\{ \left(\overline{\rho}_d \tilde{\mathbf{u}}_d \tilde{\mathbf{u}}_d \right) + \left(\overline{\rho_d \mathbf{u}''_d \mathbf{u}''_d} \right) - \tau_c \right\} = -\alpha_d \nabla p + \overline{\rho}_d g + F_d \qquad (4)$$

Where,

$$\overline{\rho}_d = (1 - \alpha_c) \rho_d = \alpha_d \rho_d$$

The momentum exchange between the two phases is represented by Stokes law and turbulent correction factor

$$F_d = \frac{18\mu_c}{\overline{d}^2} \left\{ \alpha_d \left(\mathbf{u}_c - \mathbf{u}_d \right) - \frac{1}{\overline{\alpha}_c} \gamma_{t,d} \nabla \overline{\alpha}_c \right\} \qquad (5)$$

The dispersed phase droplet size is treated as scalar transport equation given by;

$$\frac{\partial \overline{\rho}_d \overline{d}}{\partial t} + \nabla \cdot \left\{ \left(\overline{\rho}_d \tilde{\mathbf{u}}_d \cdot \overline{d} \right) - \mu_{t,d} \nabla \cdot \overline{d} \right\} = K \qquad (6)$$

The turbulent viscosity is obtained using the $k - \varepsilon$ model given by;

$$\mu_t = \overline{\rho}_c C_\mu \frac{k^2}{\varepsilon} \qquad (7)$$

Where;

C_μ=0.09;

And K represents the source term that models droplet break up and coalescence.

$$K = \overline{\rho}_d \left(\frac{\overline{d}_{eq} - \overline{d}}{\tau} \right); \qquad (8)$$

Here $\overline{d}_{eq}$ is the equilibrium droplet size that is a multivariate variable representative of the real interfacial behaviour incorporating interfacial tension, chemistry and all other effects of emulsion stability prevalent in the given system. Similarly τ is the relaxation time that is also a function of all the above effects.

Geometry and mesh

In this work the simulations were performed with Ansys Fluent 15.0 software. The geometry was developed using the design modeller. The cylindrical tank geometry of the stirred tank was created with the same dimensions as in the experiments discussed earlier. The cylindrical tank geometry is also added with internal boundaries such as baffles, impeller shaft and blades. Within this created fluid zone two separate zones of stationary and impeller zones were created where the impeller zone was the area swept by impeller. The two zones were created as two

independent bodies and parts with a common interface surface connecting them as a sliding mesh. This geometry is shown in Fig. 3.

Within the generated geometry tetrahedron mesh was generated throughout the stationary and impeller zones with a sliding mesh interface. A symmetric cut view of this is provided in Fig. 4. While generating this mesh the setting was adjusted for refinement at curvatures and sharp edges. The grid size was restricted between the minimum size of 1mm and maximum size of 5mm. The face size was restricted to 3mm.
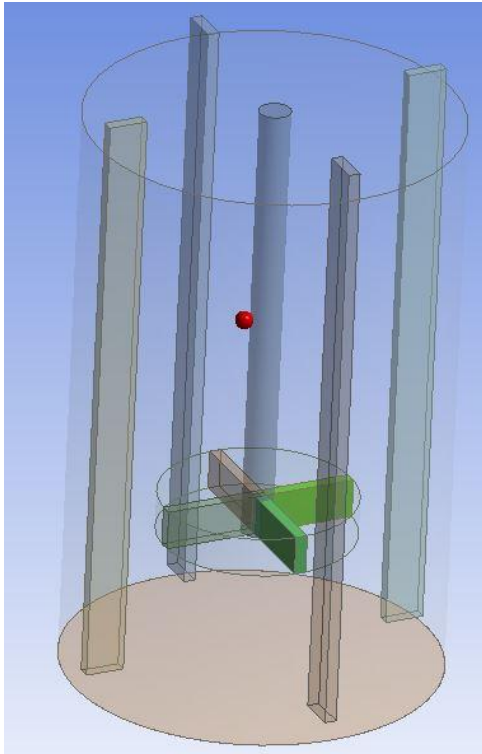
Figure 3: Geometry created using the design modeller
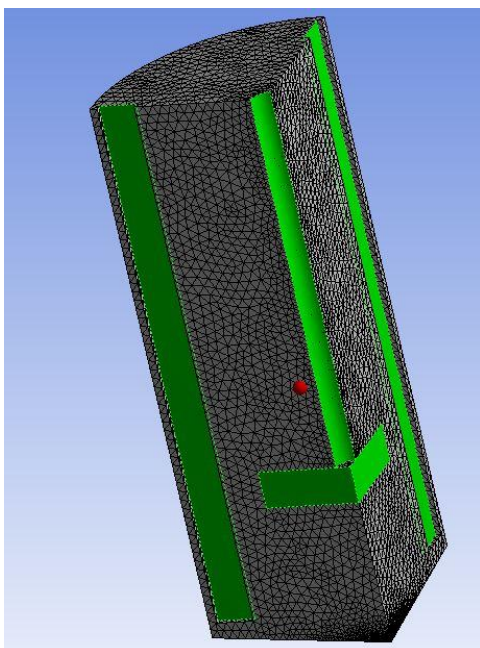
Figure 4: Cut view of the generated mesh

RESULTS

Experimental results

The PVM probes captured images of droplets in emulsions with respect to time. The frequency of image capture was set at 6s. According to Kraume et. al. (2004) work, a number of at least 300 droplets have to be counted to have a reliable distribution measurement. Therefore images are captured in sets of 4 so that enough droplets are measured. Fig. 5 shows a magnified view of a sample image. Due to the clear model oil (Nexbase) droplet interfaces are very clearly observed.

On post processing most of the droplets in focus are well detected. These detected droplets are shown in Fig. 6. The edges of droplets were detected using the Otsu (1979) method or grey threshold method. This operation gives a binary image consisting of detected edges (1) and background (0). The detected edges are used to estimate centres of circles and their radii using Hough transform method for circle detection. The features of the image processing toolbox in Matlab were used for these detections.

Figure 5: Magnified part of a raw image captured by PVM probe
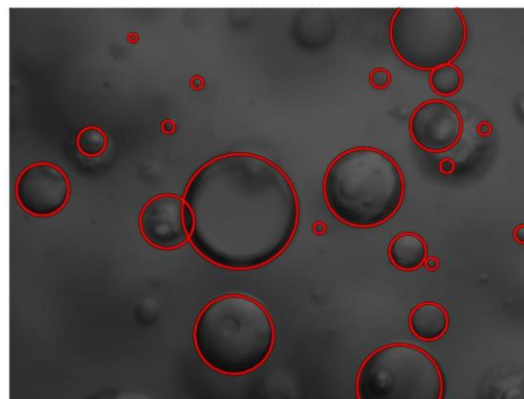
Figure 6: Processed image with detected droplets

At each of the given time interval all the detected circle data is accumulated and the Sauter mean diameter, mean diameter and standard deviation of distribution were calculated. The Sauter mean diameter, which is basically volume/surface area weighted diameter, was plotted against time. This is given by eq. 10;

4

$$\overline{d}_{SMD} = \frac{\sum \overline{d}^3}{\sum \overline{d}^2} \qquad (10)$$

As explained earlier the rotational speed and torque measured by torque sensor mounted on the impeller were also recorded with respect to time. Fig. 7 shows the plot of Sauter mean diameter and torque with respect to time simultaneously. This plot is for water in oil experimental run where the water cut is 15% by wt. As described earlier in section: Experimental methods the rotation speed was reduced in steps from 3500 RPM to 2000 RPM and then from 2000 RPM to 1000 RPM. Next it was raised back to 3500 RPM again and reduced to 1000 RPM. The time given for these steps is 120 s for high level speed and 240 s for low and medium level speeds. These time settings are chosen based on enough time needed to reach equilibrium at the respective impeller speed. Similar variations are maintained for experimental run with surfactant SPAN 80 where due to lowering of interfacial tension the droplets are smaller in size. This can be seen in Fig. 8.

These two sets of experiments clearly show that the large difference in droplet size behavior is caused by even small variation in chemistry and interfacial tension. In the same range of torque variations the droplet sizes are different and the time scales of droplet size evolution are also different. Without surfactants the droplet sizes vary from 40 μm to 150 μm and with surfactant SPAN 80 the droplet sizes varied between 10 μm and 30 μm. The largest droplet size was reached with 500 RPM speed which was lower than that used in experiments without surfactants where the largest droplet size of 150 μm are recorded at 1000 RPM.
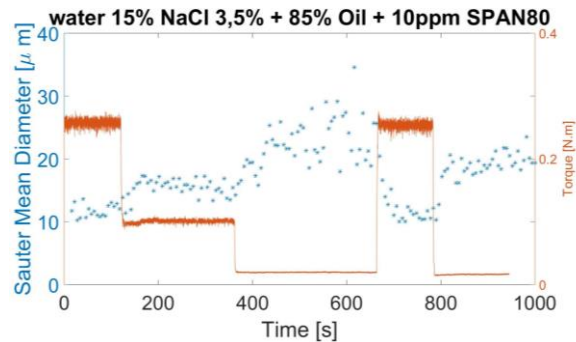
Figure 7: Sauter mean diameter and torque plotted against time for emulsion without surfactants. Here the 3 levels of rotational speed used are 3500 RPM, 2000 RPM and 1000 RPM

During high speed of rotation the system gets a high energy input that causes droplets to break up under high interfacial energy. As soon as the speed is decreased to the new level depending on the driving force the droplets start coalescing more to form larger droplets and thus reaching a new equilibrium droplet size. Depending on the interfacial stability the time scales for coalescence and equilibration are different. Due to adsorption of species such as salt, surfactants or other ingredients in the oil or water phase at the interface the coalescence of droplets are affected. This was shown previously by Pauchard and Roy (2014) in their work on jamming due to asphaltenes. In their work the effect of adsorbed asphaltenes at droplet interface is studied causing hindrance in droplet coalescence.
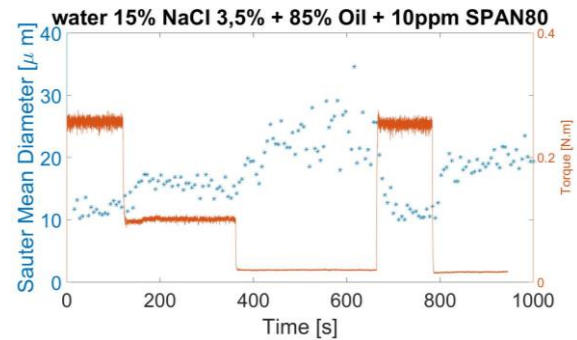
Figure 8: Sauter mean diameter and torque plotted against time for emulsion with surfactants. Here the 3 levels of rotational speed used are 2500 RPM, 1500 RPM and 500 RPM

In the current work we want to accommodate the effects of ingredients of emulsions in the droplet size evolution and equilibration. This is done using the formulation of the source term in droplet size (scalar) evolution equation shown earlier in Eq. 6. The current set of experimental results will help in providing a fundamental concept for such a study.

Simulation results

Single phase flow test case

The implementation of the geometry and meshing was needed to be tested before put to use under multi-phase flow conditions. The geometry consisted of internals such as 4 impeller flat blades. The area swept by these blades was treated as a separate zone called impeller zone. This axisymmetric zone was rotated about the vertical z direction with the rotational speed of impeller causing the blades to rotate alongside the mesh with the same speed.
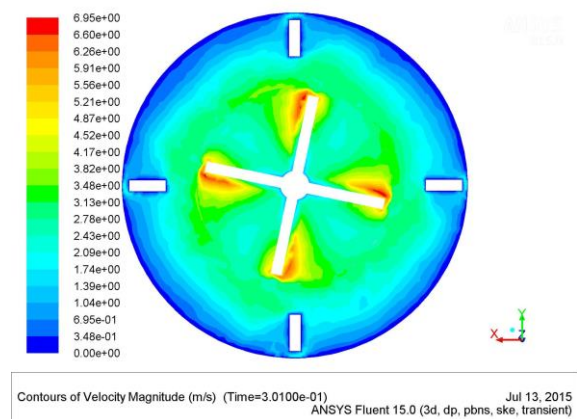
Figure 9: Cross sectional bottom view of the tank in the plane of the impeller.

In this test the impeller was rotated with the speed of 3000 RPM and the fluid flow in the horizontal plane of the impeller was observed. This is shown in Fig. 9 which is at the time 0.3 s after the start of the impeller rotation. At the given impeller speed, where the impeller diameter was 48

mm, the tip speed of the impeller is 7.5 m/s. The fluid velocity profile in Fig. 9 shows that the fluid velocity near the tip of the impeller reaches close to this velocity level. This indicates a successful implementation of the internals and sliding mesh geometry.

Multiphase flow test case

The oil-water emulsion flow was modelled with an Euler-Euler multiphase model consisting of a continuous phase and dispersed droplet phase. The droplet Sauter mean diameter of the dispersed phase was modelled as a scalar quantity. In this method the droplet size stability was modelled using a user defined stability term defined earlier by Eq. 6. This stability was implemented into the Fluent solver using a User defined function.

This implementation was tested using a simplified test case where a low turbulent viscosity coefficient (only in droplet model Eq. 6) and a low impeller speed of 200 RPM were set. Therefore, the transient droplet size became a first order direct function of the stability driving force given by Eq. 8. The entire domain was initiated with a dispersed volume fraction of 0.15. The equilibrium droplet size $\bar{d}_{eq}$ was set to 0.1mm and the initial droplet size $\bar{d}_{init}$ was set at 1 mm. This obviously implies a droplet break up leading to the new equilibrium.
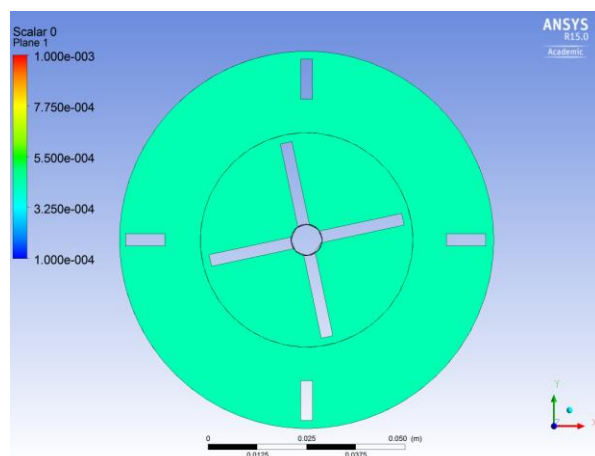
Figure 10: Sauter mean droplet size for time t = 0.01 s.
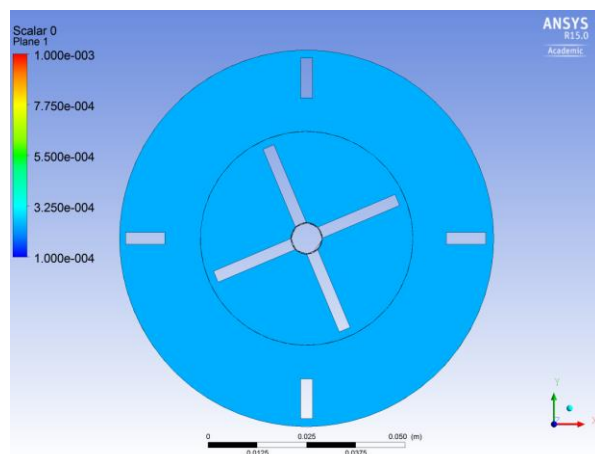
Figure 11: Sauter mean droplet size for time t = 0.02 s.

For this test case the relaxation time constant τ was arbitrarily fixed as 0.01 s for verification purpose. A first order dynamic system reaches 63% of the equilibration value and at two times the time constant it reaches 86% of equilibration value. Thus closely agreeing with these values the droplet size reached 0.4 mm and 0.2 mm at times 0.01 s and 0.02 s respectively. This is shown in Fig. 10 and Fig 11 which are for these respective simulation times.

It can also be noticed that due to a low turbulent viscosity coefficient for droplets and low inertial forces the droplet sizes are uniform throughout the domain. This was done just for the purpose of this test so that a first order transient variation is observed. With this verification test a successful implementation of the multiphase model was made. This model is now ready for experimental validation with droplet size emulsion stability.

CONCLUSION

A flat blade stirred tank set up with PVM probe was designed and fabricated. Images of droplet size evolution was captured and post processed with a newly developed imaging technique. Using the developed technique droplets size variation with respect to varying rotation speed of the impeller was obtained. These characterization experiments were done with and without surfactants in model Nexbase oil as continuous phase and water as dispersed phase. The experiments showed the sharp difference in equilibrium droplet size and relaxation times by a mere 10 ppm addition of surfactants. These experiments produced surface chemistry based droplet size stability results that can be used for CFD validations.

An Euler-Euler based model was developed where the dispersed phase droplet size was treated as a scalar. This model was implemented in Fluent solver using flat blade geometry internals and sliding mesh method was adopted. The implementation was tested with single phase flow where the fluid velocity at the blade tip was matched to be close to the tip speed itself. Further multiphase implementation of the scalar droplet size was also verified for a simplified case where at one and two times time constant the droplet size reached 63% and 86% of the equilibrium value. The CFD model is ready as a tool to understand and describe the dynamic droplet stability of a given system.

REFERENCES

KOLMOGOROV, A., (1949), "On the disintegration of drops in a turbulent flow", *Dok. Akad. Nauk.,* **66,** 825-828.

BOXALL J. A., KOH C. A., SLOAN E. D., SUM A. K., and WU D. T., (2010), "Measurement and calibration of droplet size distributions in water-in-Oil emulsions by particle video microscope and a focused beam reflectance method", *Ind. and Engg. Chem. Res.,* **49**, 1412-1418.

BOXALL, J. A, KOH, C. A, SLOAN, E. D., SUM, A. K., and WU, D. T., (2012), "Droplet size scaling of water-in-oil emulsions under turbulent flow", *Langmuir: The ACS Journal of Surfaces and Colloids*, **28**, 104-10.

GREAVES, D., BOXALL, J., MULLIGAN, J., MONTESI, A., CREEK, J., SLOAN, E. D. and KOH, C. A., (2008), "Measuring the Particle Size of a Known

Distribution using the Focused Beam Reflectance Measurement Technique", *Chem. Engg. Sci.*, **63**, 5410-5419.

ABIDIN M. I. I. Z., RAMAN A. A. A., and NOR M. I. M., (2013), "Review on measurement techniques for drop size distribution in a stirred vessel", *Ind. and Engg. Chem. Res.*, **52** (46), 16085-16094.

WYNN E.J.W., (2003), "Relationship between particle-size and chord-length distributions in focused beam reflectance measurement: stability of direct inversion and weighting", *Powder Technology* **133**, 125-133.

KEMPKES M., EGGERS J., and MAZZOTTI M., (2008), "Measurement of particle size and shape by FBRM and in situ microscopy", *Chem. Engg. Sci.*, **63** (19), 4656-4675.

LAUX H., and JOHANSEN S.T., (1999), "A CFD analysis of the air entrainment rate due to a plunging steel jet combining mathematical models for dispersed and separated multiphase flows", *Fluid Flow Phenomena in Metal Processing, Edited by N. El-Kaddah et al., The Minerals, Metals and Materials Society*, 21-30.

GOHEL S., JOSHI S., AZHAR M., HORNER M., and PADRON G., (2012), "CFD modelling of solid suspension in a stirred tank: effect of drag models and turbulent dispersion on cloud height", *International Journal of Chemical Engineering, Article ID 956975*, 1-9.

CIOFALO, M., BRUCATO A., and GRISAFI F., TORRACA N., (1996), "Turbulent flow in closed and free-surface unbaffled tanks stirred by radial impellers", *Chem. Engg. Sci.,* **51** (14), 3557-3573.

MURTHY B.N., GHADGE R.S. and JOSHI, J.B., (2007), "CFD simulations of gas–liquid–solid stirred reactor: Prediction of critical impeller speed for solid suspension", *Chem. Engg. Sci.*, **62** (24), 7184-7195.

MURTHY B.N., and JOSHI J.B., (2008), "Assessment of standard, RSM and LES turbulence models in a baffled stirred vessel agitated by various impeller designs", *Chem. Engg. Sci.*, **63** (22), 5468-5495.

MCCABE W.L., SMITH J.C. and HARRIOTT P., (2002), "Unit Operations of Chemical Engineering", McGraw Hill, Chemical Engineering Series, Sixth Edition.

KRAUME M., GABLER A., and SCHULZE K., (2004), "Influence of physical properties on drop size distributions of stirred liquid–liquid dispersions", *Chem. Engg. Tech.* **27** (3), 330-334.

OTSU N., (1979), "A Threshold Selection Method from Gray-Level Histograms", *IEEE Transactions on Systems, Man, and Cybernetics*, **9** (1), 62-66.

YUEN H. K., PRINCEN J., ILLINGWORTH J., and KITTLER J., (1990), "Comparative study of Hough transform methods for circle finding", *Image and Vision Computing*, **8** (1), 71-77.

PAUCHARD V., and ROY T., (2014), "Blockage of coalescence of water droplets in asphaltenes solutions: A jamming perspective", *Colloids and Surfaces A: Physicochem. Engg. Aspects*, **443,** 410-417.